SUPPLEMENTAL INFORMATION (SI)

Requirement of Essential Pbp2x and GpsB for Septal Ring Closure in *Streptococcus pneumoniae* D39

Adrian D. Land[†1], Ho-Ching T. Tsui[†*1], Ozden Kocaoglu[2], Stephen Vella[1], Sidney L. Shaw[1], Susan K. Keen[1], Lok-To Sham[1], Erin E. Carlson[2,3], and Malcolm E. Winkler*[1]

Departments of Biology[1], Molecular and Cellular Biochemistry[2], and Chemistry[3], Indiana University Bloomington,

Bloomington, IN 47405

[†]Contributed equally to this work.*Co-corresponding authors.

*Co-corresponding authors

Table S1. Bacterial strains used in this study[a]

***S. pneumoniae* strains**			
Strain number	Genotype (description)[b]	Antibiotic resistance[c]	Reference or source
E177	D39 Δ*cps* Δ*pbp1a*::P_c-e*rm* (IU1945 transformed with fusion amplicon Δ*pbp1a*::P_c-e*rm*)	Erm^R	(Land & Winkler, 2011)
E180	D39 Δ*cps* Δ*pbp2a*::P_c-*erm* (IU1945 transformed with fusion amplicon Δ*pbp2a*::P_c-e*rm*)	Erm^R	(Land & Winkler, 2011)
E193	D39 Δ*cps* Δ*pbp1b*::P_c-*erm* (IU1945 transformed with fusion amplicon Δ*pbp1b*::P_c-e*rm*)	Erm^R	(Land & Winkler, 2011)
IU1945	D39 Δ*cps*	None	(Lanie *et al.*, 2007)
IU3238	R6 *mreC*-L-$FLAG^3$- P_c-*erm*	Erm^R	(Land & Winkler, 2011)
IU4846	D39 Δ*cps* Δ*bgaA*::*kan*-t1t2-P_{fcsK}-*gpsB* (IU1945 transformed with fusion Δ*bgaA*::*kan*-t1t2-P_{fcsK}-*gpsB* amplicon)	Kan^R	This study
IU4888	D39 Δ*cps* Δ*gpsB*<>*aad9*//Δ*bgaA*::*kan*-t1t2-P_{fcsK}-*gpsB* (IU4846 transformed with fusion Δ*gpsB*<>*aad9* amplicon)	Kan^R Spc^R	This study
IU4970	D39 Δ*cps mreC*-L-$FLAG^3$- P_c-*erm*	Erm^R	(Land & Winkler, 2011)
IU4972	D39 Δ*cps* Δ*pbp2a*::P_c-*erm* Δ*gpsB*<>*aad9*// Δ*bgaA*::*kan*-t1t2-P_{fcsK}-*gpsB* (IU4888 transformed with Δ*pbp2a*::P_c-*erm* amplicon from E180)	Kan^R Erm^R Spc^R	This study
IU4974	D39 Δ*cps* Δ*pbp1b*::P_c-*erm* Δ*gpsB*<>*aad9*//Δ*bgaA*::*kan*-t1t2-P_{fcsK}-*gpsB* (IU4888 transformed with Δ*pbp1b*::P_c-*erm* amplicon from E193)	Kan^R Erm^R Spc^R	This study
IU4976	D39 Δ*cps* Δ*gpsB*<>*aad9*//Δ*bgaA*::*kan*-t1t2-P_{fcsK}-*gpsB mreC*-L-$FLAG^3$-P_c-e*rm* (IU4888 transformed with *mreC*-L-$FLAG^3$-P_c-e*rm* amplicon from IU3238)	Kan^R Erm^R Spc^R	This study
IU4978	D39 Δ*cps* Δ*pbp1a*::P_c-e*rm* Δ*gpsB*<>*aad9*//Δ*bgaA*::*kan*-t1t2-P_{fcsK}-*gpsB* (IU4888 transformed with	Kan^R Erm^R Spc^R	This study

	Δ*pbp1a*::P_c-e*rm* amplicon from E177)		
IU5458	D39 Δ*cps gpsB*-L-FLAG^3-P_c-e*rm* (IU1945 transformed with fusion *gpsB*-L-FLAG^3-P_c-e*rm* amplicon)	Erm^R	This study
IU5544	D39 Δ*cps pbp1a*-L-FLAG^3-P_c-e*rm* (IU1945 transformed with fusion *pbp1a*-L-FLAG^3-P_c-e*rm* amplicon)	Erm^R	This study
IU5838	D39 Δ*cps gpsB*-FLAG-P_c-e*rm* (IU1945 transformed with fusion *gpsB*-FLAG-P_c-e*rm* amplicon)	Erm^R	This study
IU5840	D39 Δ*cps pbp1a*-FLAG-P_c-e*rm* (IU1945 transformed with fusion *pbp1a*-FLAG-P_c-e*rm* amplicon)	Erm^R	This study
IU5846	D39 Δ*cps* Δ*gpsB*<>*aad9*//Δ*bgaA*::*kan*-t1t2-P_{fcsK}-*gpsB* (IU4846 transformed with Δ*gpsB*<>*aad9* amplicon from IU4888)	Kan^R Spc^R	This study
IU5847	D39 Δ*cps* Δ*gpsB*<>*aad9*//Δ*bgaA*::*kan*-t1t2-P_{fcsK}-*gpsB* (IU4846 transformed with Δ*gpsB*<>*aad9* amplicon from IU4888)	Kan^R Spc^R	This study
IU5980	D39 Δ*cps* Δ*gpsB*<>*aad9*//Δ*bgaA*::*kan*-t1t2-P_{fcsK}-*gpsB pbp1a*-FLAG-P_c-e*rm* (IU4888 transformed with *pbp1a*-FLAG-P_c-e*rm* amplicon from IU5840)	Kan^R Erm^R Spc^R	This study
IU6506	D39 Δ*cps pbp2x*-L-FLAG^3-P_c-erm (IU1945 transformed with fusion *pbp2x*-L-FLAG^3-P_c-*erm* amplicon)	Erm^R	This study
IU6565	D39 Δ*cps ftsZ*-FLAG-P_c-*erm* (IU1945 transformed with fusion *ftsZ*-FLAG-P_c-*erm* amplicon)	Erm^R	This study
IU6570	D39 Δ*cps ftsZ*-Myc-P_c-erm (IU1945 transformed with fusion *ftsZ*-Myc-P_c-*erm* amplicon)	Erm^R	This study
IU6819	D39 Δ*cps pbp2x*-FLAG^3-P_c-erm (IU1945 transformed with fusion *pbp2x*-FLAG^3-P_c-*erm* amplicon)	Erm^R	This study
IU6929	D39 Δ*cps pbp2x*-HA-P_c-*kan* (IU1945 transformed with fusion *pbp2x*-HA-P_c-*kan*)	Kan^R	This study
IU6944	D39 Δ*cps* Δ*gpsB*<>*aad9*//Δ*bgaA*::*kan*-t1t2-P_{fcsK}-*gpsB ftsZ*-FLAG-P_c-*erm* (IU4888 transformed with *ftsZ*-FLAG-	Kan^R Erm^R Spc^R	This study

	P_c-e*rm* amplicon from IU6565)		
IU6946	D39 Δ*cps* Δ*gpsB*<>*aad9*//Δ*bgaA*::*kan*-t1t2-P_{fcsK}-*gpsB ftsZ*-Myc-P_c-e*rm* (IU4888 transformed with *ftsZ*-Myc-P_c-e*rm* amplicon from IU6570)	Kan^R Erm^R Spc^R	This study
IU6962	D39 Δ*cps ftsZ*-Myc-P_c-*kan* (IU1945 transformed with fusion *ftsZ*-Myc-P_c-*kan* amplicon)	Kan^R	This study
IU6964	D39 Δ*cps gpsB*-FLAG-P_c-*erm ftsZ*-Myc-P_c-*kan* (IU5838 transformed with fusion *ftsZ*-Myc-P_c-*kan* amplicon)	Kan^R Erm^R	This study
IU6976	D39 Δ*cps ftsZ*-Myc-P_c-*kan pbp1a*-FLAG-P_c-*erm* (IU6962 transformed with *pbp1a*-FLAG-P_c-*erm* amplicon from IU5840)	Kan^R Erm^R	This study
IU6978	D39 Δ*cps ftsZ*-Myc-P_c-*kan pbp2x*-$FLAG^3$-P_c-*erm* (IU6962 transformed with *pbp2x*-$FLAG^3$-P_c-*erm* amplicon from IU6819)	Kan^R Erm^R	This study
IU6980	D39 Δ*cps* Δ*gpsB*<>*aad9*//Δ*bgaA*::*kan*-t1t2-P_{fcsK}-*gpsB pbp2x*-$FLAG^3$-P_c-e*rm* (IU4888 transformed with *pbp2x*-$FLAG^3$-P_c-e*rm* amplicon from IU6819)	Kan^R Erm^R Spc^R	This study
IU7199	D39 *Δcps gpsB*-Myc-P_c-*erm* (IU1945 tranformed with fusion *gpsB*-Myc-P_c-*erm* amplicon)	Erm^R	This study
IU7365	D39 Δ*cps pbp2x*-HA-P_c-*kan pbp1a*-L-$FLAG^3$-P_c-*erm* (IU5544 transformed with *pbp2x*-HA-P_c-*kan* amplicon from IU6929)	Kan^R Erm^R	This study

[a]Strains were constructed as described in *Experimental procedures*.

[b]Primers used to synthesize fusion amplicons are listed in Supplemental Table S2. All FLAG-tagged (FLAG), c-Myc-tagged (Myc), and HA-tagged (HA) fusions were made to the carboxyl-ends of reading frames. The amino acid sequence for the FLAG epitope is DYKDDDDK (Hopp *et al*., 1988; Wayne *et al.*, 2010). $FLAG^3$ indicates three tandem sequences of the FLAG epitope and L refers to a 10-amino-acid spacer linker

(GSAGSAAGSG) (Waldo *et al*., 1999; Wayne *et al*., 2010)). The amino acid sequence of the c-Myc epitope is EQKLISEEDL (Evan *et al.*, 1985), and the amino acid sequence of the HA epitope is YPYDVPDYA (Tu *et al*. 2008).

[c]Antibiotic resistance markers: Erm^R, erythromycin; Kan^R, kanamycin; Spc^R, spectinomycin.

SUPPLEMENTAL TABLE S2. Oligonucleotide primers used in this study (order follows Table S1)

Primer	Sequence (5' to 3')	Template[a]	Amplicon Product
For construction of E177 (Δ*pbp1a*::P_c-*erm*)			
P234	CCCTTGTGTTCATAGCGAGGATAAGCA	D39	5' upstream fragment with 60nt of 5' *pbp1a*
P236	CATTATCCATTAAAAATCAAACGGATCCTACA AGCTTAAGAAGCTAATGCTCAGATACTT		
Kan rpsL forward	TAGGATCCGTTTGATTTTTAATGGATAATG	P_c-*erm* cassette[b]	P_c-*erm*
Kan rpsL reverse	GGGCCCCTTTCCTTATGCTTTTG		
P237	CAAAAGCATAAGGAAAGGGGCCCCAACAATC AAATACAACCCCTGATCAACAAAATC	D39	60 nt of 3' *pbp1a* and 3' downstream fragment
P235	AGGCAAGCCTGCAACCATGGTCTTGAAA		
For construction of E180 (Δ*pbp2a*::P_c-*erm*)			
P226	GGTACGACAACGAAATGTCATACACTGCAC	D39	5' upstream fragment with 60nt of 5' *pbp2a*
P228	CATTATCCATTAAAAATCAAACGGATCCTATT CACTTGTTTCTTTTTTAAAAAGAGAAAG		
Kan rpsL forward	TAGGATCCGTTTGATTTTTAATGGATAATG	P_c-*erm* cassette[b]	P_c-*erm*
Kan rpsL reverse	GGGCCCCTTTCCTTATGCTTTTG		
P229	CAAAAGCATAAGGAAAGGGGCCCGCGAAGA TTAAGGAAAAGGCTCAAACAATATG	D39	60 nt of 3' *pbp2a* and 3' downstream fragment
P227	TCTGTTCCCGTGTGATCCGACAAATCCT		
For construction of E193 (Δ*pbp1b*::P_c-*erm*)			
P222	CGTTCGTGTGGCGCTGCTTCAAATTGTT	D39	5' upstream fragment with 100nt of 5' *pbp1b*
P456	CATTATCCATTAAAAATCAAACGGATCCTATT GAACCTTTCTTGCCAGGTCTAGCTGATT		
Kan rpsL forward	TAGGATCCGTTTGATTTTTAATGGATAATG	P_c-*erm* cassette[b]	P_c-*erm*
Kan rpsL reverse	GGGCCCCTTTCCTTATGCTTTTG		
P225	CAAAAGCATAAGGAAAGGGGCCCTCTAGCGA TAGCAGTAACTCAAGTACTACACGACCTT	D39	60 nt of 3' *pbp1b* and 3' downstream fragment
P223	ACTGGCACTGATAACGGCAACCACCAAA		

For construction of IU4846 (Δ*bgaA*::P_c-*kan* t1t2-P_{fcsK}-*gpsB*)			
KG067	TCTTGTCGGTGTGTTGAAAATTATCAACTC	IU3348[c]	*bgaA'*-P_c-*kan*t1t2-P_{fcsk}
AL310	TAATACTTGCCATTTTTCTTCTCTCTTCGTCC		
AL311	GAGAGAAGAAAAATGGCAAGTATTATTTT TTCAG	D39	*gpsB*
AL312	GTAAGTTCTTTTATTAAAAATCTGAGTTATC		
AL313	CTCAGATTTTTAATAAAAGAACTTACTTTC	IU3348[c]	*bgaA*'
XX043	GGCTATCTTCTCCACTATCTACCACAG		
For construction of IU4888 (Δ*gpsB*<>*aad9*)			
AL298	GAGGGAAGGCACCAGCCTTGATTTCA	D39	5'-flanking fragment
AL314	CAAATATATCCTCCTCACGTCTCTCTCCATTC		
AL315	CTAGCAAGCGAGAATGGAGAGAGACGT GAGGAGG	IU3931[d]	*aad9*
AL317	CTCAAATAACTACTAATTTTTTTAATCTG		
AL316	GATTAAAAAAATTAGTAGTTATTTGAGAT GTGC	D39	3'-flanking fragment
AL301	CGTTTAAAGAGGCTAGACCCGGTCGTATC		
For construction of IU5458 (*gpsB*-L-FLAG^3-P_c-*erm*)			
TT196	GCCAAGCCCTGAGACAAATAGTAGTCGTTGGT	D39	5'-flanking fragment
TT198	CGGAGCCAGCGGAACCAAAATCTGAGTTATCT AAAATTTGTTTACCAAAAAC		
AL355	CTCAGATTTTGGTTCCGCTGGCTCCG	IU3238[e]	L-FLAG^3-P_c-*erm*
TT199	AAATTGCACATCTCAAATAACTACTTTCCTCCC GTTAAATAATAGATAACTATTAAAAAT		
TT200	TAGTTATCTATTATTTAACGGGAGGAAAGTAGT TATTTGAGATGTGCAATTTTTGGATAA	D39	3'-flanking fragment
TT197	TTTGATACGATCTGCTGCCCGAAGCCAAAGGT		
For construction of IU5544 (*pbp1a*-L-FLAG^3-P_c-*erm*)			
TT225	AGCCGTGGAAACTCTAAACAAGGTCGGACT	D39	5'-flanking fragment
TT226	CGGAGCCAGCGGAACCTGGTTGTGCTGGTTG AGGATTCTG		
AL304	CCAGCACAACCAGGTTCCGCTGGCTCCGC	IU3238[e]	L-FLAG^3-P_c-*erm*
TT227	CAGAAAAATCTGGATGATAAATGTTATTTCCTC CCGTTAAATAATAGATAACTATTAAAA		
TT228	TAGTTATCTATTATTTAACGGGAGGAAATAACA TTTATCATCCAGATTTTTCTGGGTG	D39	3'-flanking fragment
P235	AGGCAAGCCTGCAACCATGGTCTTGAAA		
For construction of IU5838 (*gpsB*-FLAG-P_c-*erm*)			
TT196	GCCAAGCCCTGAGACAAATAGTAGTCGTTGGT	D39	5'-flanking fragment
TT262	TTATTTATCATCATCATCTTTATAATCAAAATCT GAGTTATCTAAAATTTGTTTACCAAA		

TT263	TAACTCAGATTTTGATTATAAAGATGATGATGA TAAATAACCGGGCCCAAAATTTGTTTG	IU5458[f]	3'-flanking fragment
TT197	TTTGATACGATCTGCTGCCCGAAGCCAAAGGT		
For construction of IU5840 (*pbp1a*-FLAG-P_c-*erm*)			
TT225	AGCCGTGGAAACTCTAAACAAGGTCGGACT	D39	5'-flanking fragment
TT264	TGGGCCCGGTTATTTATCATCATCATCTTTATA ATCTGGTTGTGCTGGTTGAGGATTCTG		
TT265	ACCAGCACAACCAGATTATAAAGATGATGATG ATAAATAACCGGGCCCAAAATTTGTTTG	IU5544[f]	3'-flanking fragment
P235	AGGCAAGCCTGCAACCATGGTCTTGAAA		
For construction of IU6506 (*pbp2x*-L-FLAG^3-P_c-*erm*)			
TT345	GTGACCCAGACGCAAATGATTCGTGCCTTT	D39	5'-flanking fragment
TT347	CGGAGCCAGCGGAACCGTCTCCTAAAGTTAA TGTAATTTTTTTAATGTCCTTG		
TT348	CATTAAAAAAATTACATTAACTTTAGGAGACG GTTCCGCTGGCTCCGC	IU5544[f]	L-FLAG^3-P_c-*erm*
TT349	CTGATGGAAATAAACATATTATTATTTCCTCC CGTTAAATAATAGATAACTATTAAAAAT		
TT350	ATAGTTATCTATTATTTAACGGGAGGAAATAA TAATATGTTTATTTCCATCAGTGCTGGA	D39	3'-flanking fragment
TT346	AGAAGTCAACCTTCCACTCGCTCCAAGGAT		
For construction of IU6565 (*ftsZ*-FLAG-P_c-*erm*)			
TT165	AGTGGTGCCGATATGGTCTTCATCACTGCT	IU4368[g]	5'-flanking fragment
TT369	AAATTTTGGGCCCGGTTATTTATCATCATCAT CTTTATAATCACGATTTTTG		
TT370	CACCTCCATTTTTCAAAAATCGTGATTATAAA GATGATGATGATAAATAACCGGG	IU4368[g]	3'-flanking fragment
TT166	TCATTGGGAGAGCCGGTTCCTGTGAAGAAT		
For construction of IU6570 (*ftsZ*-Myc-P_c-*erm*)			
TT165	AGTGGTGCCGATATGGTCTTCATCACTGCT	IU4368[g]	5'-flanking fragment
TT371	TAAAGATCTTCTTCAGAAATAAGTTTTTGTTCA CGATTTTTGAAAAATGGAGGTGTATCC		
TT372	AATCGTGAACAAAAACTTATTTCTGAAGAAGA TCTTTAACCGGGCCCAAAATTTGTTTGA	IU4368[g]	3'-flanking fragment
TT166	TCATTGGGAGAGCCGGTTCCTGTGAAGAAT		
For construction of IU6819 (*pbp2x*-FLAG^3-P_c-*erm*)			
TT345	GTGACCCAGACGCAAATGATTCGTGCCTTT	D39	5'-flanking fragment

SV026	TTTATCATCATCATCTTTATAATCGTCTCCTAA AGTTAATGTAATTTTTTTAATGTCC		
SV027	AAAATTACATTAACTTTAGGAGACGATTATAA AGATGATGATGATAAA	IU6506[f]	3'-flanking fragment
TT346	AGAAGTCAACCTTCCACTCGCTCCAAGGAT		
For construction of IU6929 (*pbp2x*-HA-P_c-*kan*)			
TT345	GTGACCCAGACGCAAATGATTCGTGCCTTT	D39	5'-flanking fragment
SV034	GCATAATCTGGAACATCATATGGATAGTCTCC TAAAGTTAATGTAATTTTTTTAATGTCC		
SV035	ATTAAAAAAATTACATTAACTTTAGGAGACTAT CCATATGATGTTCCAGATTATGCTTAA	IU6810[h]	HA-P_c-*kan*
SV036	CAGCACTGATGGAAATAAACATACTAAAACAA TTCATCCAGTAAAATATAATATTTTATT		
SV037	AATATTATATTTTACTGGATGAATTGTTTTAGT ATGTTTATTTCCATCAGTGCTGGAATT	D39	3'-flanking fragment
TT346	AGAAGTCAACCTTCCACTCGCTCCAAGGAT		
For construction of IU6962 and IU6964 (*ftsZ*-Myc-P_c-*kan*)			
TT165	AGTGGTGCCGATATGGTCTTCATCACTGCT	IU6570[f]	5'-flanking-fragment
SV046	CGGTGATATTCTCATTTTAGCCATGTAATCAC TCCTTCTTAATTACAAATTTTTAGCAT		
SV047	AAAAATTTGTAATTAAGAAGGAGTGATTACAT GGCTAAAATGAGAATATCACCGGA	P_c-*kan*-*rpsL*$^+$ cassette[b]	Kan ORF
SV048	CTGTATTTTCTTTTACATTCATTTACCTAAAAC AATTCATCCAGTAAAATATAATATTTT		
SV049	TATATTTTACTGGATGAATTGTTTTAGGTAAAT GAATGTAAAAGAAAATACAGAACTTGT	D39	3'-flanking fragment
TT166	TCATTGGGAGAGCCGGTTCCTGTGAAGAAT		
For construction of IU7199 (IU1945 *gpsB*-Myc-P_c-*erm*)			
TT196	GCCAAGCCCTGAGACAAATAGTAGTCGTTGGT	D39	5'-flanking-fragment
TT422	TCTTCTTCAGAAATAAGTTTTTGTTCAAAATCT GAGTTATCTAAAATTTGTTTACCAAAA		
TT423	AACAAATTTTAGATAACTCAGATTTTGAACAAA AACTTATTTCTGAAGAAGATCTTTAAC	IU6570[f]	Myc-P_c-*erm*
TT199	AAATTGCACATCTCAAATAACTACTTTCCTCCC GTTAAATAATAGATAACTATTAAAAAT		
TT200	TAGTTATCTATTATTTAACGGGAGGAAAGTAGT TATTTGAGATGTGCAATTTTTGGATAA	D39	3'-flanking-fragment

AL301	CGTTTAAAGAGGCTAGACCCGGTCGTATC		

[a]Genomic DNA of the indicated *S. pneumoniae* strains was used as templates for PCR reactions, except for P_c-*erm* cassettes.

[b]P_c-*erm* and P_c-*kan-rpsL*$^+$ cassettes are described in (Tsui *et al.*, 2011).

[c]Genotype of IU3348 is R6 Δ*bgaA'*::P_c-*kan*t1t2-P_{fcsK}-*pcsB*-L-FLAG^3 (Wayne *et al*., 2010).

[d]Genotype of IU3931 is D39 Δ*cps* Δ*mreCD*<>*aad9*//Δ*bgaA*::*kan*-t1t2-P_{fcsK}-*mreCD* (Land & Winkler, 2011).

[e]Genotype of IU3238 is R6 *mreC*-L-FLAG^3-P_c-*erm* (Land & Winkler, 2011).

[f]Strain from this study.

[g]Genotype of IU4368 is D39 Δ*cps ftsZ*-FLAG^3-P_c-*erm* (Tsui *et al*., 2011).

[h]IU6810 is an unpublished laboratory strain.

SUPPLEMENTAL MOVIE LEGENDS

Movie S1. Dual FtsZ and GpsB IFM of strain IU6964 (*ftsZ*-Myc *gpsB*-FLAG) imaged using 3D-SIM showing Y-axis rotation of the two cells in Fig. 3B (a). FtsZ and GpsB staining are represented by red and green signals, respectively.

Movie S2. Dual FtsZ and Pbp2x IFM of cells of strain IU6978 (*ftsZ*-Myc *pbp2x*-FLAG^{3}) imaged using 3D-SIM showing X-axis rotation of the middle section of the cell in Fig.4B (a). FtsZ and Pbp2x staining are represented by red and green signals, respectively.

Movie S3. Dual FtsZ and Pbp1a IFM of cells of strain IU6976 (*ftsZ*-Myc *pbp1a*-FLAG) imaged using 3D-SIM showing Y-axis rotation of the cell in Fig. 5B (a). FtsZ, Pbp1a, and DAPI staining are represented by red, green, and blue signals, respectively.

Movie S4. Dual Pbp2x and Pbp1a IFM of cells of strain IU7365 (*pbp2x*-HA *pbp1a*-L-FLAG^{3}) imaged using 3D-SIM showing X-axis rotation of the late-divisional cell in Fig. 6B (d). Pbp2x, Pbp1a, and DAPI staining are represented by red, green, and blue signals, respectively.

Movie S5. Multiple FtsZ rings shown by IFM of strain IU6944 (Δ*gpsB//*P$_{fcsK}$-*gpsB ftsZ*-FLAG) depleted of GpsB in BHI broth lacking fucose. Images were obtained by 3D-SIM and show Y-axis rotation of the cell in Fig. 7A (bottom). FtsZ and DAPI staining are represented by green and blue signals, respectively.

Movie S6. Multiple Pbp1a rings shown by IFM of cells of strain IU5980 (Δ*gpsB//*P$_{fcsK}$-*gpsB*$^{+}$ *pbp1a*-FLAG*)* depleted for GpsB in BHI broth lacking fucose. Images were obtained by 3D-SIM and show Y-axis rotation of the cell in Fig. 7B

(bottom). Pbp1a and DAPI staining are represented by green and blue signals, respectively.

REFERENCES

Evan, G.I., G.K. Lewis, G. Ramsay & J.M. Bishop, (1985) Isolation of monoclonal antibodies specific for human c-myc proto-oncogene product. *Molec and Cell Biol* **5**: 3610-3616.

Hopp, T. P., K. S. Prickett, V. L. Price, R. T. Libby, C. J. March, D. P. Cerretti, D. L. Urdal, and P. J. Conlon**,** (1988). A short polypeptide marker sequence useful for recombinant protein identification and purification. *Biotechnology (NY)* **6:**1204-1210.

Land, A.D. & M.E. Winkler, (2011) The requirement for pneumococcal MreC and MreD is relieved by inactivation of the gene encoding PBP1a. *J Bacteriol* **193**: 4166-4179.

Lanie, J.A., W.L. Ng, K.M. Kazmierczak, T.M. Andrzejewski, T.M. Davidsen, K.J. Wayne, H. Tettelin, J.I. Glass & M.E. Winkler, (2007) Genome sequence of Avery's virulent serotype 2 strain D39 of *Streptococcus pneumoniae* and comparison with that of unencapsulated laboratory strain R6. *J Bacteriol* **189**: 38-51.

Tsui, H.C., S.K. Keen, L.T. Sham, K.J. Wayne & M.E. Winkler, (2011) Dynamic distribution of the SecA and SecY translocase subunits and septal localization of the HtrA surface chaperone/protease during *Streptococcus pneumoniae* D39 cell civision. *mBio* **2**(5). pii: e00202-11. doi: 10.1128/mBio.00202-11.

Tu, Y., F. Li, , & C. Wu, (2008) Nck-2, a novel Src homology2/3-containing adaptor protein that interacts with the LIM-only protein PINCH and components of growth factor receptor kinase-signaling pathways. *Mol. Bio. Cell* **9**: 3367-3382.

Waldo, G. S., B. M. Standish, J. Berendzen, and T. C. Terwilliger, (1999). Rapid protein-folding assay using green fluorescent protein. *Nat. Biotechnol* **17:**691-695

Wayne, K.J., L.T. Sham, H.C. Tsui, A.D. Gutu, S.M. Barendt, S.K. Keen & M.E. Winkler, (2010) Localization and cellular amounts of the WalRKJ (VicRKX) two-component regulatory system proteins in serotype 2 *Streptococcus pneumoniae*. *J Bacteriol* **192**: 4388-4394.

SUPPLEMENTAL FIGURE LEGENDS

Fig. S1. Time course of cell morphological changes during GpsB depletion in *S. pneumoniae* D39. Strain IU4888 (Δ*gpsB*//P_{fcsK}-*gpsB*$^{+}$) (Table S1) was grown exponentially in BHI broth containing 1.0% (wt/vol) fucose to OD_{620} ≈0.1, washed, and resuspended to OD_{620} ≈0.03 in BHI broth containing 1.0% (wt/vol) or no fucose as described in *Experimental procedures*. (A) Growth curves of strain IU4888 following resuspension in BHI broth containing or lacking fucose. Arrows indicate when samples were taken from cultures lacking fucose and correspond to the images in B. (B) Representative images of cells of strain IU4888 after 20 min, 1h 10 min, 2h, 3h, and 4h without fucose (scale bar = 1 μm). (C) Box-and-whisker plots (whiskers, 5 and 95 percentile) of cell lengths (top) and widths (bottom) of parent strain IU1945 (D39 Δ*cps gpsB*$^{+}$) and strain IU4888 depleted of GpsB. Cells were measured as described in *Experimental procedures*. Column 1, separated, pre-divisional cells IU1945 grown exponentially in BHI broth; column 2, pre-divisional cells of IU4888 grown exponentially in BHI containing fucose; column 3, pre-divisional cells of IU4888 grown exponentially in BHI containing fucose, washed with BHI, and grown in BHI containing fucose for 1.5 h (washing control); columns 4 to 6, separated cells of IU4888 grown exponentially in BHI containing fucose, washed with BHI, and resuspended in BHI without fucose for 1, 2 or 3 h. 70 or more cells from at least 3 microscope fields were measured for each condition. P values were obtained by one-way ANOVA analysis (GraphPad Prism, nonparametric Kruskal-Wallis test). The median cell lengths and widths of the IU4888 –f 1h, –f 2h, and –f 3h samples were significantly different ($p<0.05$) from those of the

IU4888 + fucose sample. Independent experiments confirmed that cells of IU4888 limited for fucose for 2 and 3h or 2.5 h had median lengths and widths similar to those in the graphs, which were significantly ($p<0.05$) larger than IU4888 grown with fucose (data not shown).

Fig. S2. GpsB is essential for growth of *S. pneumoniae* D39. IU4888 (Δ*gpsB*//P_{fcsK}-*gpsB*$^{+}$) was grown overnight in BHI broth containing 0.8% (wt/vol) fucose, washed, and resuspended to $OD_{620} \approx 0.005$ in BHI broth containing 0.1% or 0.8% (wt/vol) or no fucose as described in *Experimental procedures*. This was a different limitation protocol than the one used for Fig. 1 and S1 (see the text). The IU1945 parent (D39 Δ*cps gpsB*$^{+}$) was grown without fucose for comparison. (A) Growth curves of strain IU1945 or IU4888 depleted for GpsB. Arrows indicate when samples were taken for staining and microscopy. Prolonged incubation of IU4888 in medium lacking fucose led to the accumulation of suppressors in some cultures (data not shown). (B) Representative images of IU1945 grown to mid-log phase (OD_{620} ≈0.15), stained with FL-V, and observed by phase-contrast (Phase) and epifluorescent microscopy (FL-V) (see *Experimental procedures*). (C) Representative images of elongated, enlarged cells containing multiple rings of FL-V staining caused by depletion of GpsB (scale bar = 1 μm). Images of IU4888 cells in 0.1% (wt/vol) fucose or no fucose are representative of ≈50% of the observed cells. The elongated IU4888 cell in 0.8% (wt/vol) fucose (lower row) was far less prevalent (≈5%) than normal looking cells (top row). The experiment was performed twice with similar results.

Fig. S3. Deletion of pneumococcal Class A PBPs does not relieve lethality of GpsB depletion. Strains IU4888 (Δ*gpsB*//P_{fcsK}-*gpsB*$^{+}$), IU4978 (IU4888 Δ*pbp1a*), IU4974 (IU4888 Δ*pbp1b*), and IU4972 (IU4888 Δ*pbp2a*) were grown overnight in BHI broth containing 0.8% (wt/vol) fucose, washed, and resuspended to OD_{620} ≈0.005 in BHI broth containing 0.8% (wt/vol) or no fucose as described in *Experimental procedures*. See the text for additional details.

Fig. S4. Representative graphs showing inhibition of Boc-FL labeling of different PBPs after 30 min treatments with different doses of cefotaxime (A and B) or piperacillin (C and D) in PBS at 25ºC (A and C) or in BHI broth at 37 ºC (B and D). Strain IU1945 (D39 Δ*cps*) was grown to mid-exponential phase in BHI broth, treated with cefotaxime or piperacillin for 30 min at the indicated concentrations, and labeled with Boc-FL as described for Fig. 2 and in *Experimental procedures*.

Fig. S5. Representative images of strain IU1945 (D39 Δ*cps*) grown to exponential phase before (A), 40 min after (B), and 60 min after (C) addition of 0.1 µg/ml methicillin. Cells were stained with FL-V and DAPI as described in *Experimental procedures* and observed by phase-contrast (Phase) or epifluorescent microscopy. Scale bar = 1 µm. (D) Box-and-whisker plots (whiskers, 5 and 95 percentile) of cell lengths (left) and widths (right) of IU1945 before and at indicated times after treatment with methicillin at 0.1 µg/ml. Cell dimensions were determined as described in *Experimental procedures.* The total number of cells measured were 20 for t = 0, 16 for t = 15 min, and >25 for the other time points from at least three microscopic fields. P values were obtained by one-way ANOVA analysis (GraphPad Prism, nonparametric Kruskal-Wallis test). The

median values of cell lengths and widths for the 38, 51, 71 and 93 min samples were significantly larger ($p<0.05$) than the median lengths and widths of cells in the 0 min sample, which had similar dimensions to IU1945 cells in Fig. S1C, based on a large sample size. Independent experiments confirmed that IU1945 cells treated with 0.1 µg/ml methicillin for 50 or 60 min had median lengths and widths similar to those in the graphs, which were significantly larger ($p<0.05$) than for untreated cells (data not shown).

Fig. S6. Phenotypes of cells expressing epitope-tagged PBPs and division proteins used in this study. Full genotypes of strains are listed in Table S1. Growth determinations, Western blotting of protein amounts, and quantification of Boc-FL labeling of PBPs were performed as described in *Experimental procedures*. **(**A) Representative growth curves of the IU1945 parent (D39 Δ*cps gpsB*$^{+}$), IU5838 (*gpsB*-FLAG), and IU5458 (*gpsB*-L-FLAG^{3}) strains. (B) Western-blot analysis of strains IU1945 (untagged parent, lane 1), IU5838 (*gpsB*-FLAG*,* lane 2), and IU5458 (*gpsB*-L-FLAG^{3}*,* lane 3). (C) Representative growth curves of IU1945 parent, IU5544 (*pbp1a*-L-FLAG^{3}), and IU5840 (*pbp1a*-FLAG). (D) Western-blot analysis of strains IU1945 (untagged parent, lane 1), IU5544 (*pbp1a*-L-FLAG^{3}, lane 2) and IU5840 (*pbp1a*-FLAG*,* lane 3). **(**E) Representative growth curves of IU1945 parent, IU6565 (*ftsZ*-FLAG), IU6819 (*pbp2x*-FLAG^{3}), IU6962 (*ftsZ*-Myc-P_c-*kan*), and IU6570 (*ftsZ*-Myc-P_c-*erm*). (F) Western-blot analysis of strains IU1945 (untagged parent, lane 1), IU6565 (*ftsZ*-FLAG, lane 2), and IU6819 (*pbp2x*-FLAG^{3}*,* lane 3). (G) Western-blot analysis of strains IU1945 (untagged parent, lane 1), IU6570 (*ftsZ*-Myc-P_c-*erm*, lane 2), and IU6962 (*ftsZ*-Myc-P_c-*kan*, lane

3). (H) Boc-FL binding to PBPs in strains IU1945 (parent), IU6819 (*pbp2x*-FLAG^3), and IU5840 (*pbp1a*-FLAG). Amounts of PBPs were normalized to Pbp3 as a loading control. The amounts of Pbp2x-FLAG^3 and Pbp1a-FLAG in the shifted bands were ≈91% and ≈92% of the amounts of untagged Pbp2x and Pbp1a in the parent strain, respectively. (I) Representative growth curves of strains IU1945 (parent) and IU6929 (*pbp2x*-HA). (J) Western-blot analysis of strains IU1945 (untagged parent, lane 1) and IU6929 (*pbp2x*-HA, lane 2). (K) Boc-FL binding to PBPs in strains IU1945 (parent), IU5544 (*pbp1a*-L-FLAG^3), IU6929 (*pbp2x*-HA), and IU7365 (*pbp1a*-L-FLAG^3- *pbp2x*-HA). Amounts of PBPs were normalized to Pbp3 as a loading control. The amounts of Pbp1a-L-FLAG^3 and Pbp2x-HA in the shifted bands were ≈98% and ≈60% of the amounts of untagged Pbp1a and Pbp2x in the parent strain, respectively. See text for additional details.

Fig. S7. Representative images of dual-protein 2D IFM of cells expressing tagged versions of (A) FtsZ and GpsB, (B) FtsZ and Pbp2x, and (C) FtsZ and Pbp1 at different stages of cell division. Strains IU6964 (*ftsZ*-Myc *gpsB*-FLAG) (A)*;* IU6978 (*ftsZ*-Myc *pbp2x*-FLAG^3 (B); and IU6976 (*ftsZ*-Myc *pbp1a*-FLAG (C) were grown to mid-exponential phase in BHI broth, and DAPI staining and 2D IFM of cells were performed as described in *Experimental procedures*. Cells at different stages of division were binned based on images from phase-contrast microscopy (column 1), and localization patterns of FtsZ (pseudo-colored red, columns 2 and 5), GpsB (A), Pbp2x(B) or Pbp1a(C) (pseudo-colored green; columns 3 and 5), DNA (DAPI stained, colored white, column 4) and superimposed signals of FtsZ and GpsB, Pbp2x or Pbp1a (yellow, column 5) were determined from images obtained by wide-field epifluorescence

196 microscopy (see *Experimental procedures*). Scale bar = 1µm. Cells in images like these
197 were binned according to division stage, and average cell shapes and fluorescent
198 intensity distributions in cells at different division stages were determined by using the
199 graphical user interface program described in *Experimental procedures* (see Fig. 3A-
200 5A). (D) Plot of cell length versus division stage obtained from the analysis of strain
201 IU6978 (*ftsZ*-Myc *pbp2x*-FLAG[3]) shown in Fig. 4A. The plot was generated by the
202 graphical user interface program (see *Experimental procedures*). Similar distributions
203 were obtained for cells in Fig. 3A, 5A, and 6A (data not shown).

204 **Fig. S8**. Presence of multiple FtsZ rings in elongated cells depleted of GpsB. (A) 2D-
205 IFM of strain IU6565 (*gpsB*$^+$ *ftsZ*-FLAG) grown to mid-exponential phase and processed
206 for IFM and DAPI staining as described in *Experimental procedures*. (B) 2D-IFM of
207 strain IU6944 (Δ*gpsB*//P$_{fcsK}$-*gpsB*$^+$ *ftsZ*-FLAG) depleted of GpsB. Overnight cultures of
208 strain IU6944 grown in BHI broth containing 1.0% (wt/vol) fucose were diluted to OD_{620}
209 ≈0.005 in fresh BHI broth containing 1.0% (wt/vol) fucose. At OD_{620} ≈0.1, cells were
210 washed, and resuspended to OD ≈0.03 in fresh BHI broth containing 1.0% (wt/vol) or no
211 fucose. DAPI staining and IFM were performed on cells 2 and 3 h after resuspension
212 (see *Experimental procedures*). FtsZ (pseudo-colored green; columns 2 and 4) and
213 DNA (DAPI) (pseudo-colored white; column 3) were obtained from epifluorescent
214 microscopy as described in *Experimental procedures.* All images are shown at the
215 same magnification (scale bar = 1 µm) and are representative of >500 cells examined
216 from multiple fields. Multiple bands of FtsZ in two GpsB-depleted cells are marked by
217 white arrowheads. Similar results were obtained for strains IU6570 (*gpsB*$^+$ *ftsZ*-Myc)

and IU6946 (Δ*gpsB*//P$_{fcsK}$-*gpsB*$^{+}$ *ftsZ*-Myc), in which *ftsZ* was tagged with Myc instead of FLAG (data not shown).

Fig. S9. Presence of multiple rings of Pbp2x in elongated cells depleted of GpsB. (A) 2D-IFM images of strain IU6819 (*gpsB*$^{+}$ *pbp2x*-FLAG[3]) grown to mid-exponential phase, and processed for DAPI staining and IFM as described in *Experimental procedures*. (B) 2D-IFM images of strain IU6890 (Δ*gpsB*//P$_{fcsK}$-*gpsB*$^{+}$ *pbp2x*-FLAG[3]) depleted of GpsB as described for Fig. S8B. Samples were processed for microscopy 2 and 3 h after cultures were resuspended in BHI broth lacking fucose. DNA (DAPI) is pseudo-colored white in column 3 and Pbp2x is pseudo-colored green in columns 2 and 4. All images are shown at the same magnification (scale bar = 1 µm) and are representative of >500 cells examined from multiple fields. The experiment was performed twice with similar results. Multiple bands of Pbp2x in two GpsB-depleted cells are marked by white arrowheads.

Fig. S10. Presence of multiple Pbp1a rings in elongated cells depleted of GpsB. (A) 2D-IFM of strain IU5840 (*gpsB*$^{+}$ *pbp1a*-FLAG) that was grown to mid-exponential phase and processed for IFM and DAPI staining as described in *Experimental procedures*. (B) 2D-IFM of strain IU5980 (Δ*gpsB*//P$_{fcsK}$-*gpsB*$^{+}$ *pbp1a*-FLAG) depleted for GpsB as described for Fig. S8B. DAPI staining and IFM were performed on cells 2 and 3 h after resuspension (see *Experimental procedures*). Pbp1a (pseudo-colored green; columns 2 and 4) and DNA (DAPI) (pseudo-colored white; column 3) were obtained from epifluorescent microscopy as described in *Experimental procedures.* All images are shown at the same magnification (scale bar = 1 µm) and are representative of >500

cells examined from multiple fields. Multiple bands of Pbp1a in two GpsB-depleted cells are marked by white arrowheads.

Fig. S11. Presence of multiple rings of MreC in cells depleted of GpsB. 2D-IFM images are shown of strain IU4976 (Δ*gpsB*//P_{fcsK}-*gpsB*$^{+}$ *mreC*-L-FLAG^{3}) resuspended in BHI broth containing or lacking fucose as described for Fig. S8B. DAPI staining and IFM were performed as described in *Experimental procedures* on cells resuspended for 2 h in BHI broth containing fucose (top row) or lacking fucose for 2 or 3 h (rows 2 and 3). DNA (DAPI) is pseudo-colored white in column 3, and MreC is pseudo-colored green in columns 2 and 4. All images are shown at the same magnification (scale bar = 1 μm) and are representative of >500 cells examined from multiple fields. The experiment was performed twice with similar results. Multiple bands of MreC in one GpsB-depleted cell are marked by white arrowheads.

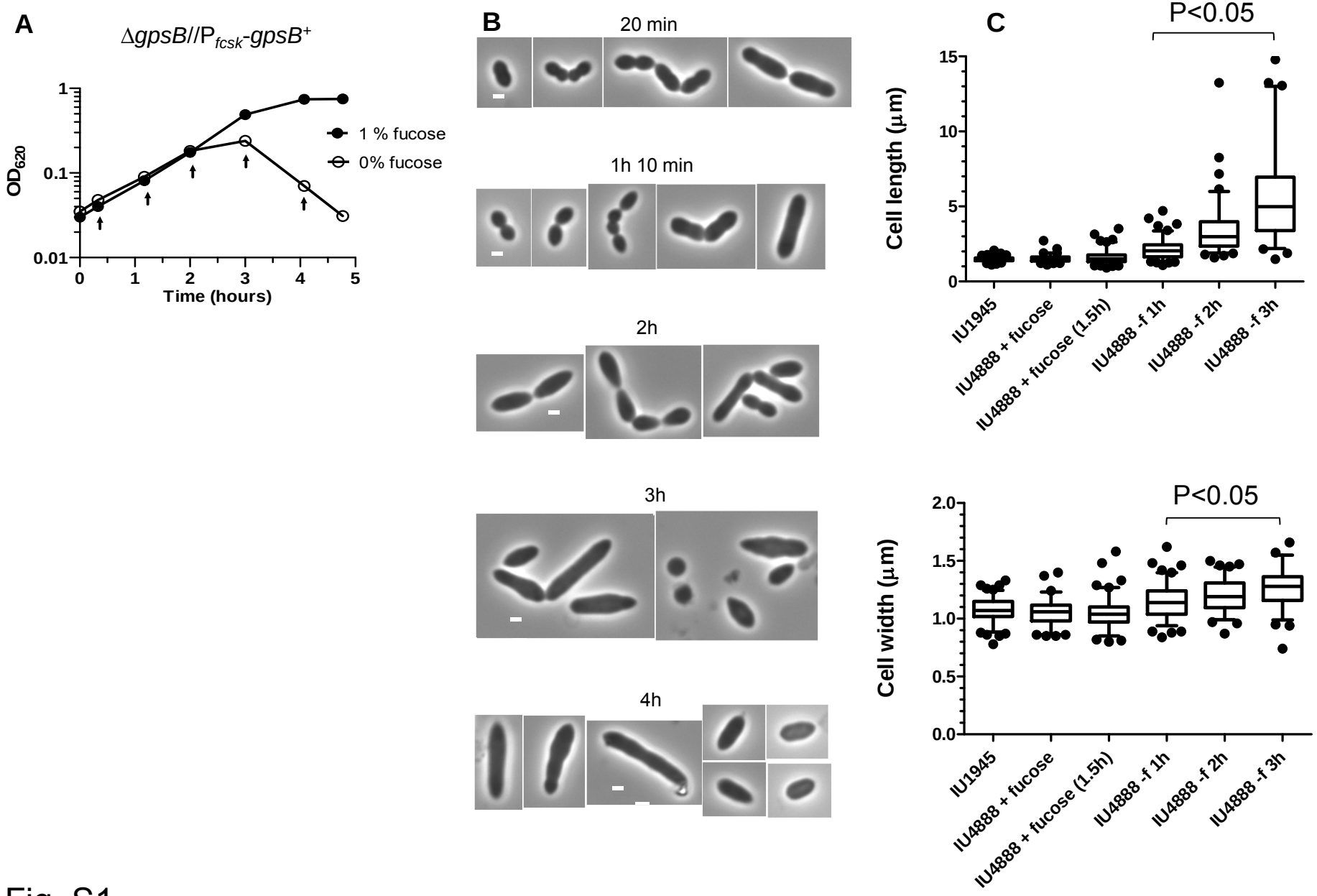
A
ΔgpsB//P fcsk-gpsB+
OD620
1
0.1
0.01
0
1
2
3
4
5
Time (hours)
1 % fucose
0% fucose
B
20 min
1h 10 min
2h
3h
4h
C
P<0.05
Cell length (µm)
15
10
5
0
IU1945
IU4888 + fucose
IU4888 + fucose (1.5h)
IU4888 -f 1h
IU4888 -f 2h
IU4888 -f 3h
P<0.05
Cell width (µm)
2.0
1.5
1.0
0.5
0.0
IU1945
IU4888 + fucose
IU4888 + fucose (1.5h)
IU4888 -f 1h
IU4888 -f 2h
IU4888 -f 3h

Fig. S1

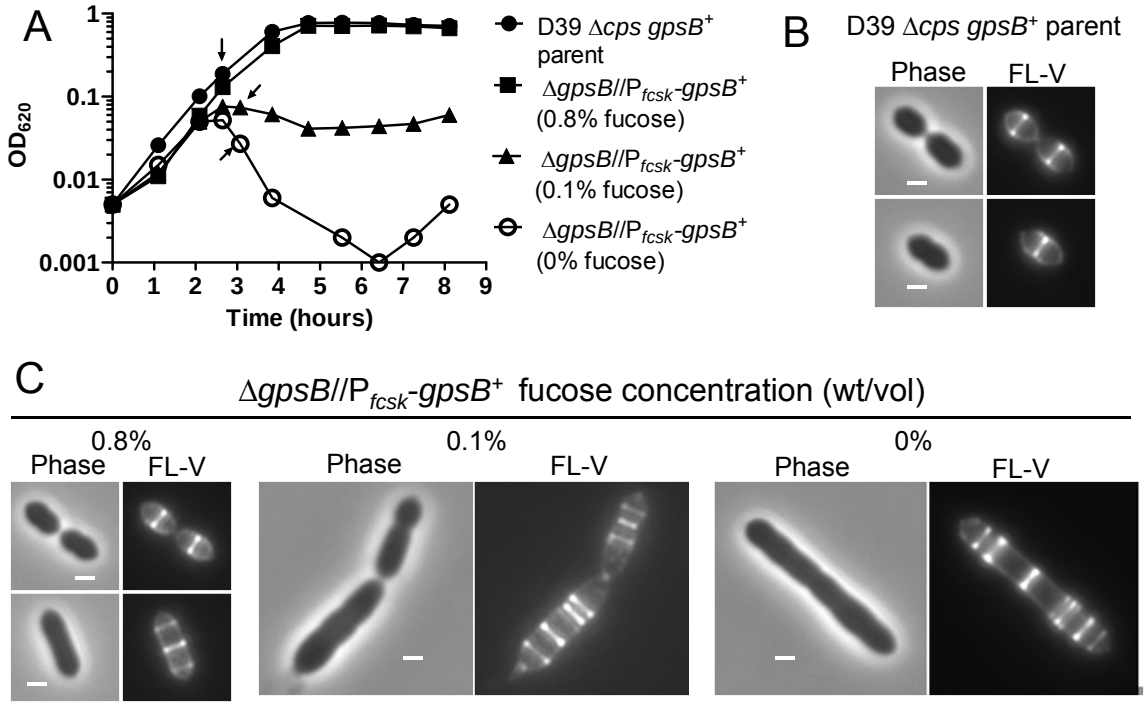
A
1
0.1
0.01
0.001
OD620
0 1 2 3 4 5 6 7 8 9
Time (hours)
D39 Δcps gpsB+ parent
ΔgpsB//Pfcsk-gpsB+ (0.8% fucose)
ΔgpsB//Pfcsk-gpsB+ (0.1% fucose)
ΔgpsB//Pfcsk-gpsB+ (0% fucose)
B
D39 Δcps gpsB+ parent
Phase
FL-V
C
ΔgpsB//Pfcsk-gpsB+ fucose concentration (wt/vol)
0.8%
0.1%
0%
Phase
FL-V

Fig. S2

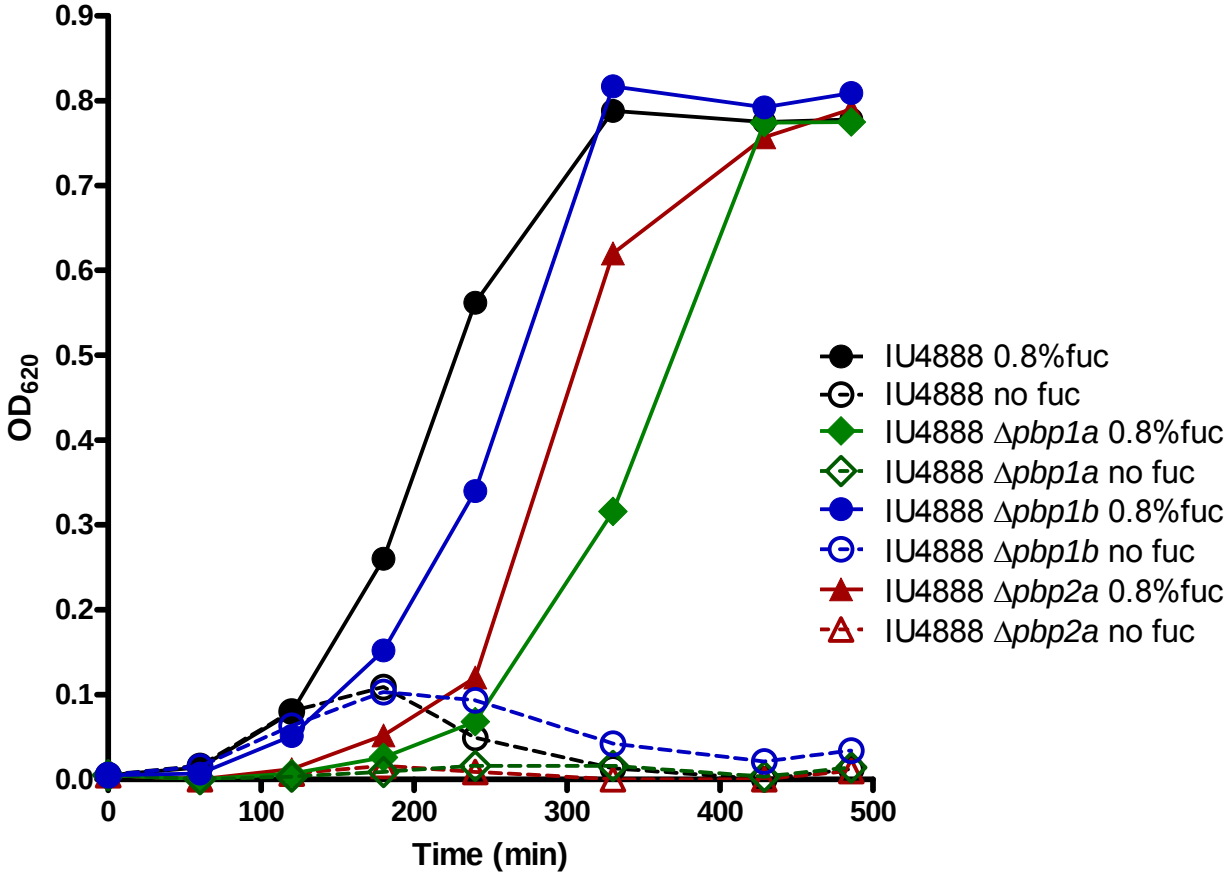
0.9
0.8
0.7
0.6
0.5
0.4
0.3
0.2
0.1
0.0
OD620
0
100
200
300
400
500
Time (min)
IU4888 0.8%fuc
IU4888 no fuc
IU4888 Δpbp1a 0.8%fuc
IU4888 Δpbp1a no fuc
IU4888 Δpbp1b 0.8%fuc
IU4888 Δpbp1b no fuc
IU4888 Δpbp2a 0.8%fuc
IU4888 Δpbp2a no fuc

Fig. S3

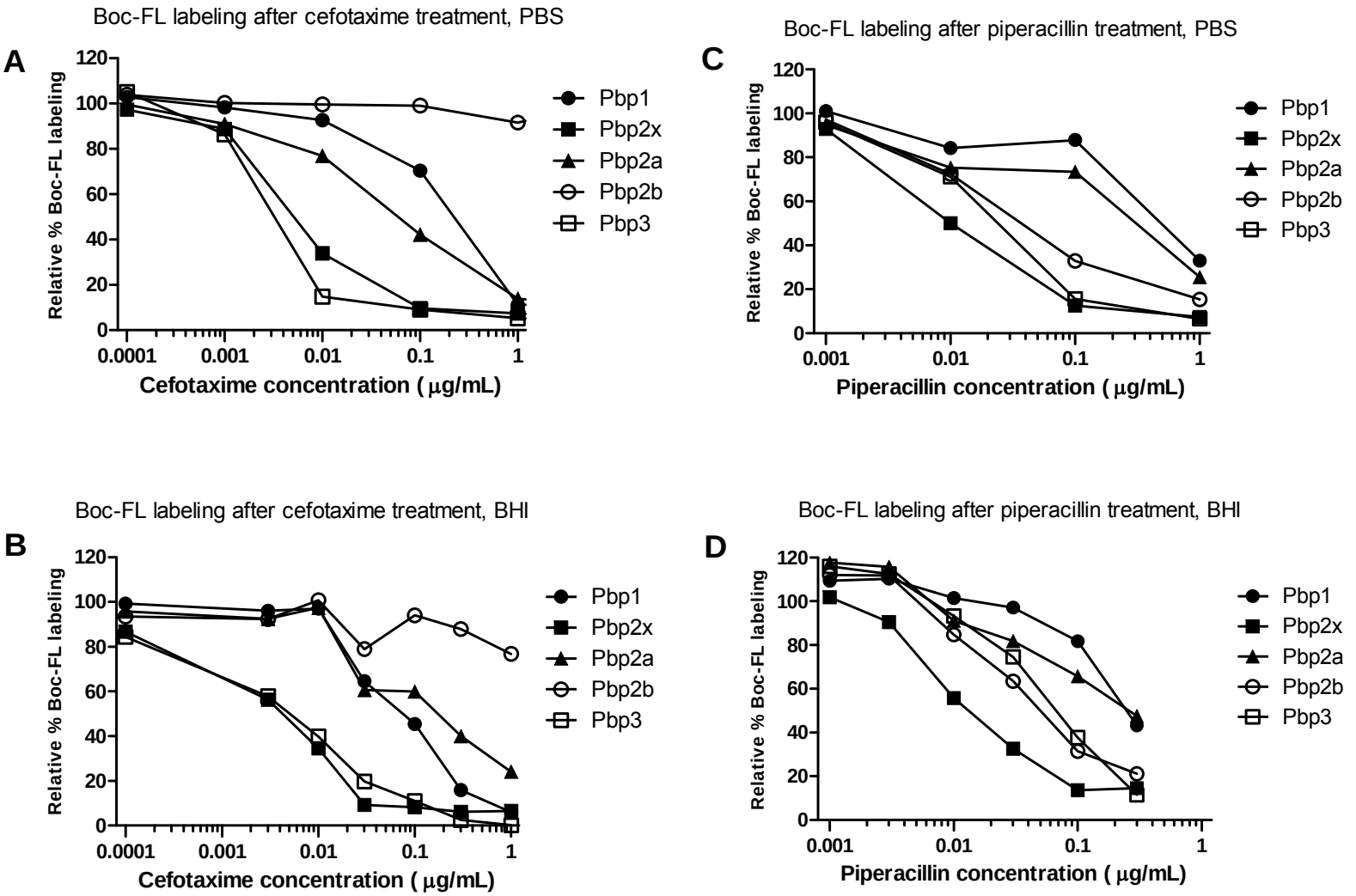
A
Boc-FL labeling after cefotaxime treatment, PBS
Relative % Boc-FL labeling
120
100
80
60
40
20
0
0.0001
0.001
0.01
0.1
1
Cefotaxime concentration (μg/mL)
Pbp1
Pbp2x
Pbp2a
Pbp2b
Pbp3
C
Boc-FL labeling after piperacillin treatment, PBS
Relative % Boc-FL labeling
120
100
80
60
40
20
0
0.001
0.01
0.1
1
Piperacillin concentration (μg/mL)
Pbp1
Pbp2x
Pbp2a
Pbp2b
Pbp3
B
Boc-FL labeling after cefotaxime treatment, BHI
Relative % Boc-FL labeling
120
100
80
60
40
20
0
0.0001
0.001
0.01
0.1
1
Cefotaxime concentration (μg/mL)
Pbp1
Pbp2x
Pbp2a
Pbp2b
Pbp3
D
Boc-FL labeling after piperacillin treatment, BHI
Relative % Boc-FL labeling
120
100
80
60
40
20
0
0.001
0.01
0.1
1
Piperacillin concentration (μg/mL)
Pbp1
Pbp2x
Pbp2a
Pbp2b
Pbp3

Fig. S4

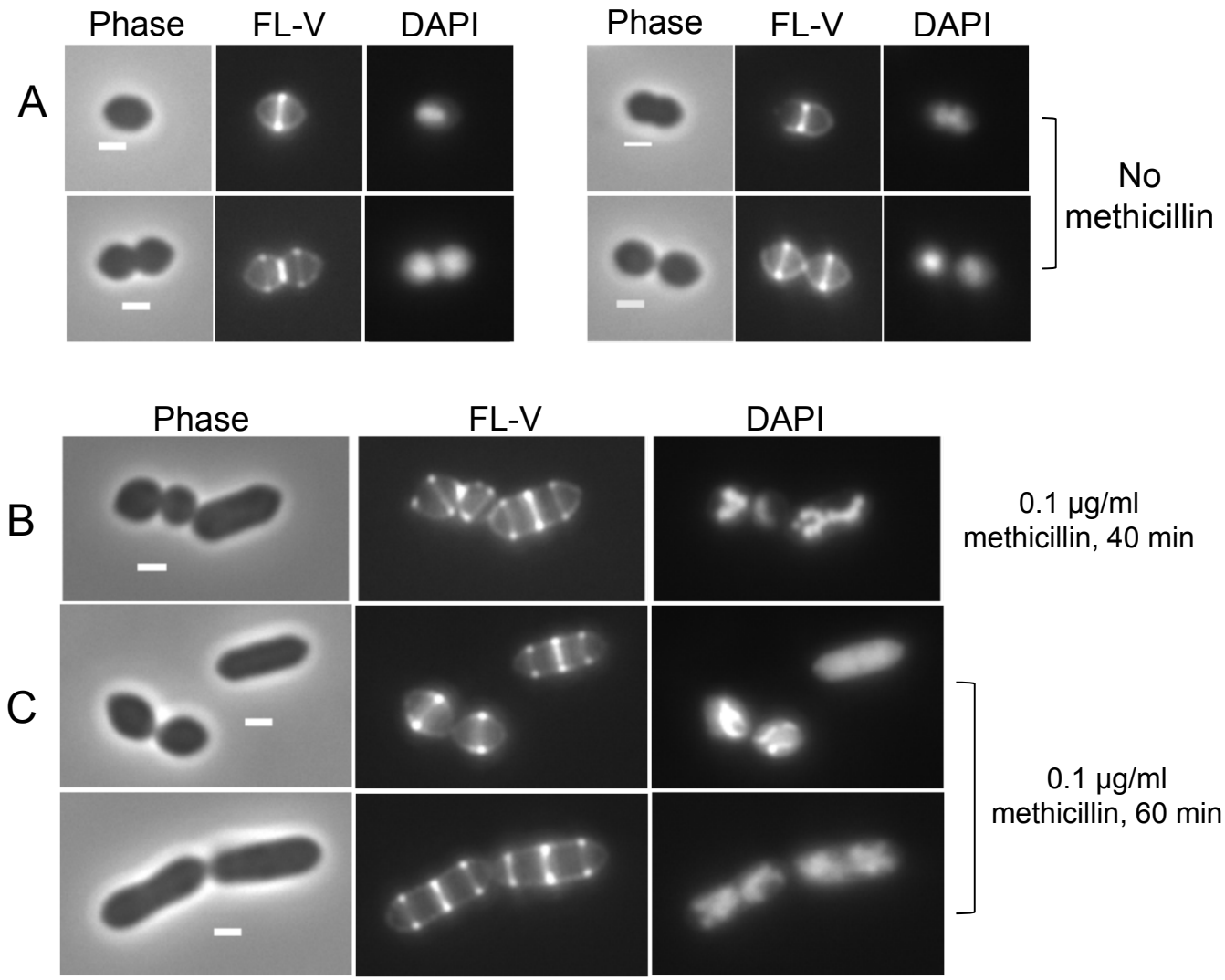

Fig. S5 (continued on next page)

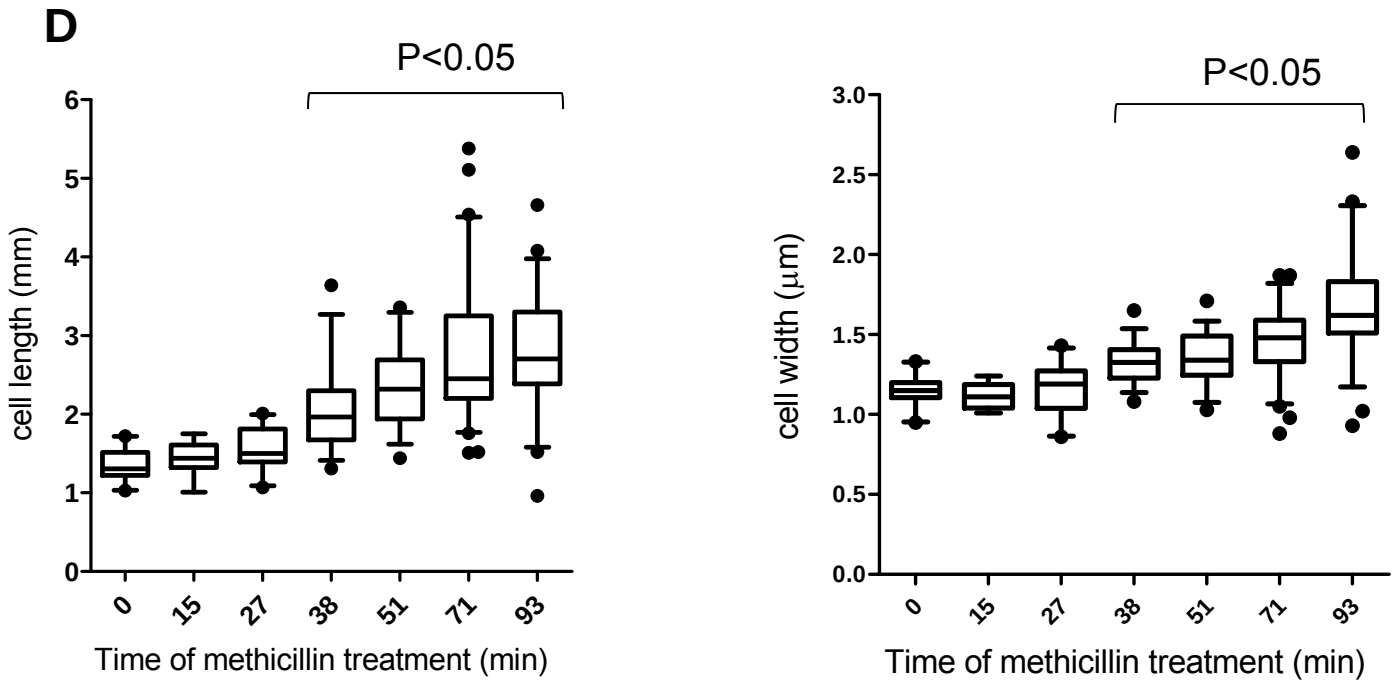

Fig. S5 (continued)

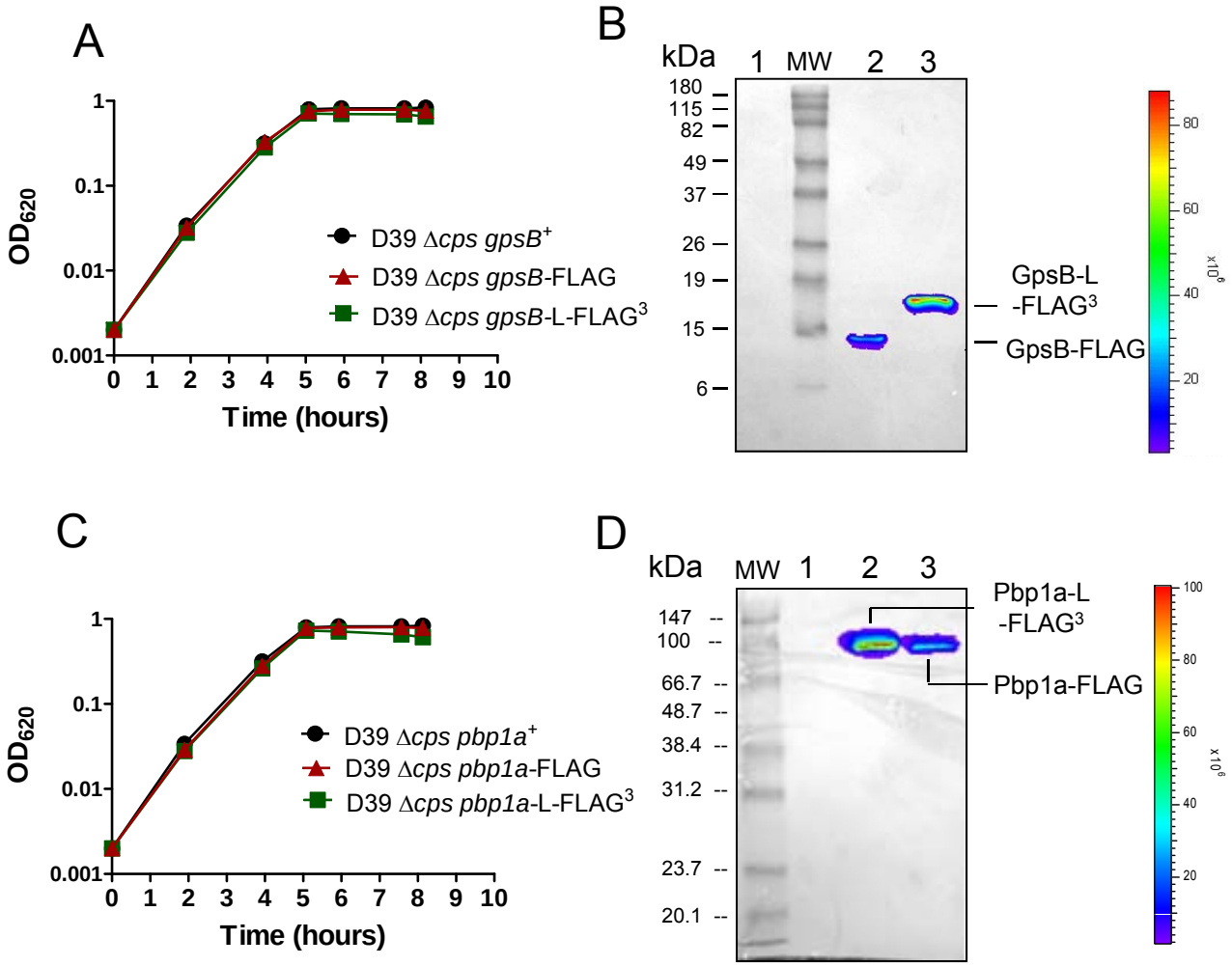

Fig. S6 (continued on next pages)

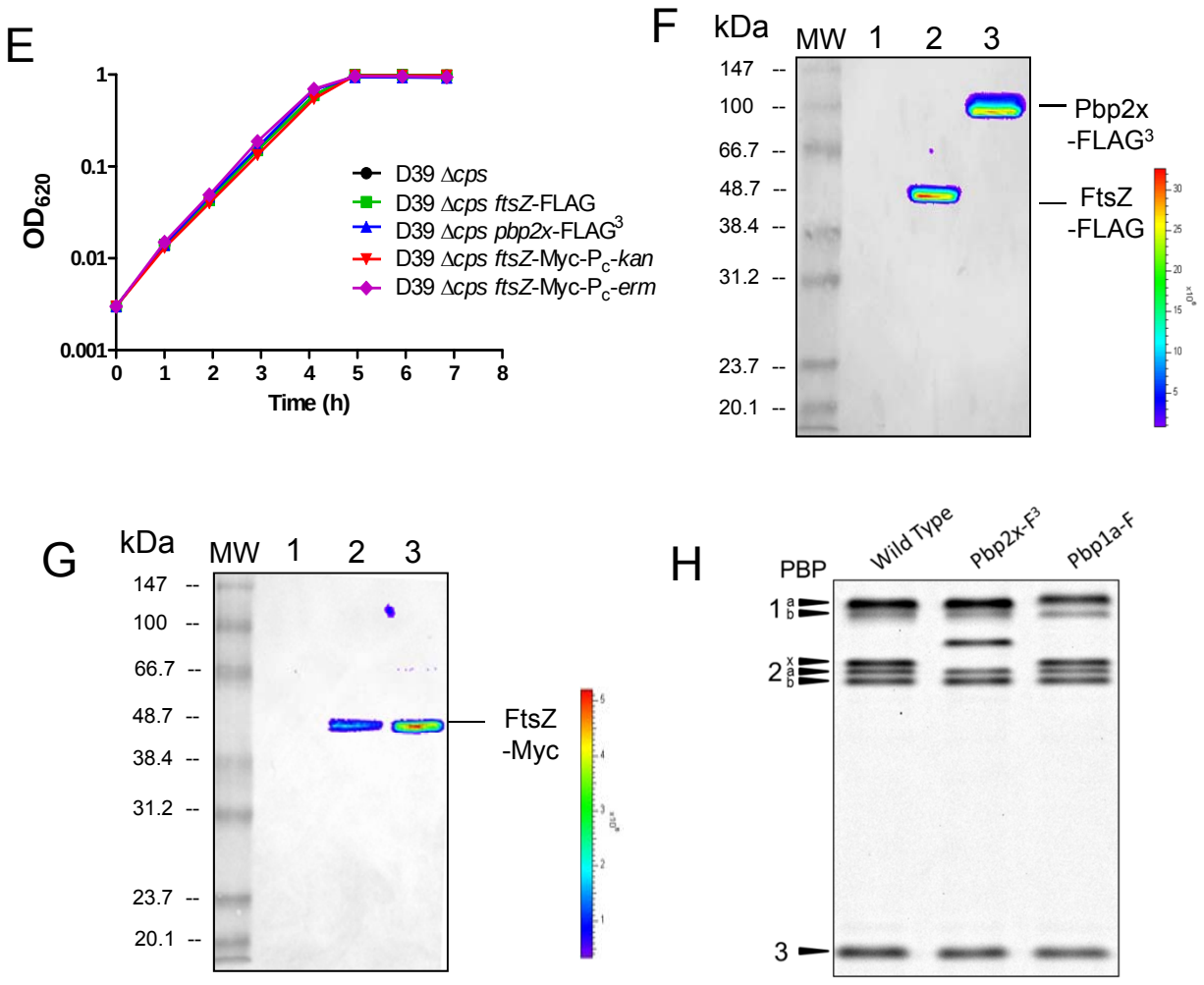

Fig. S6 (continued on next page)

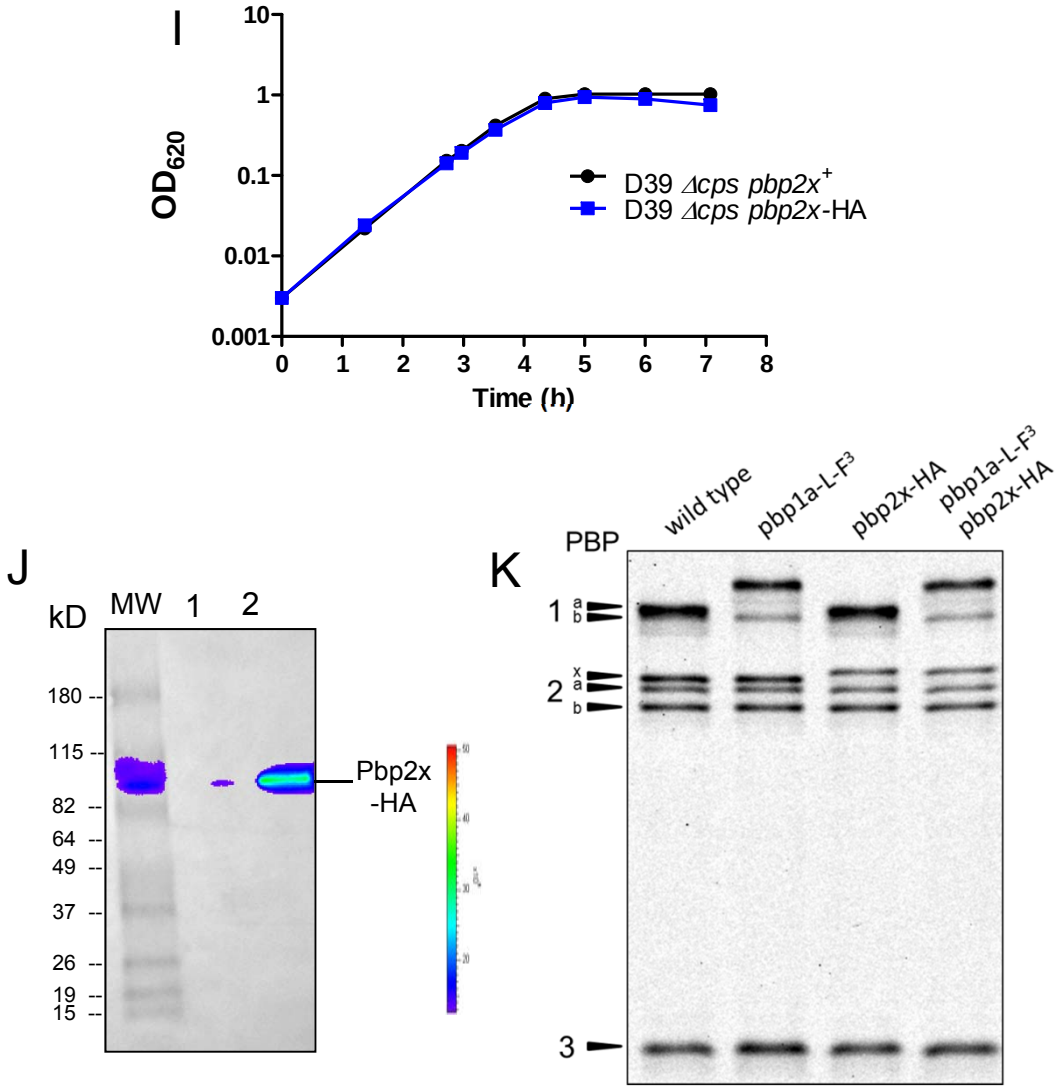

Fig. S6 (continued)

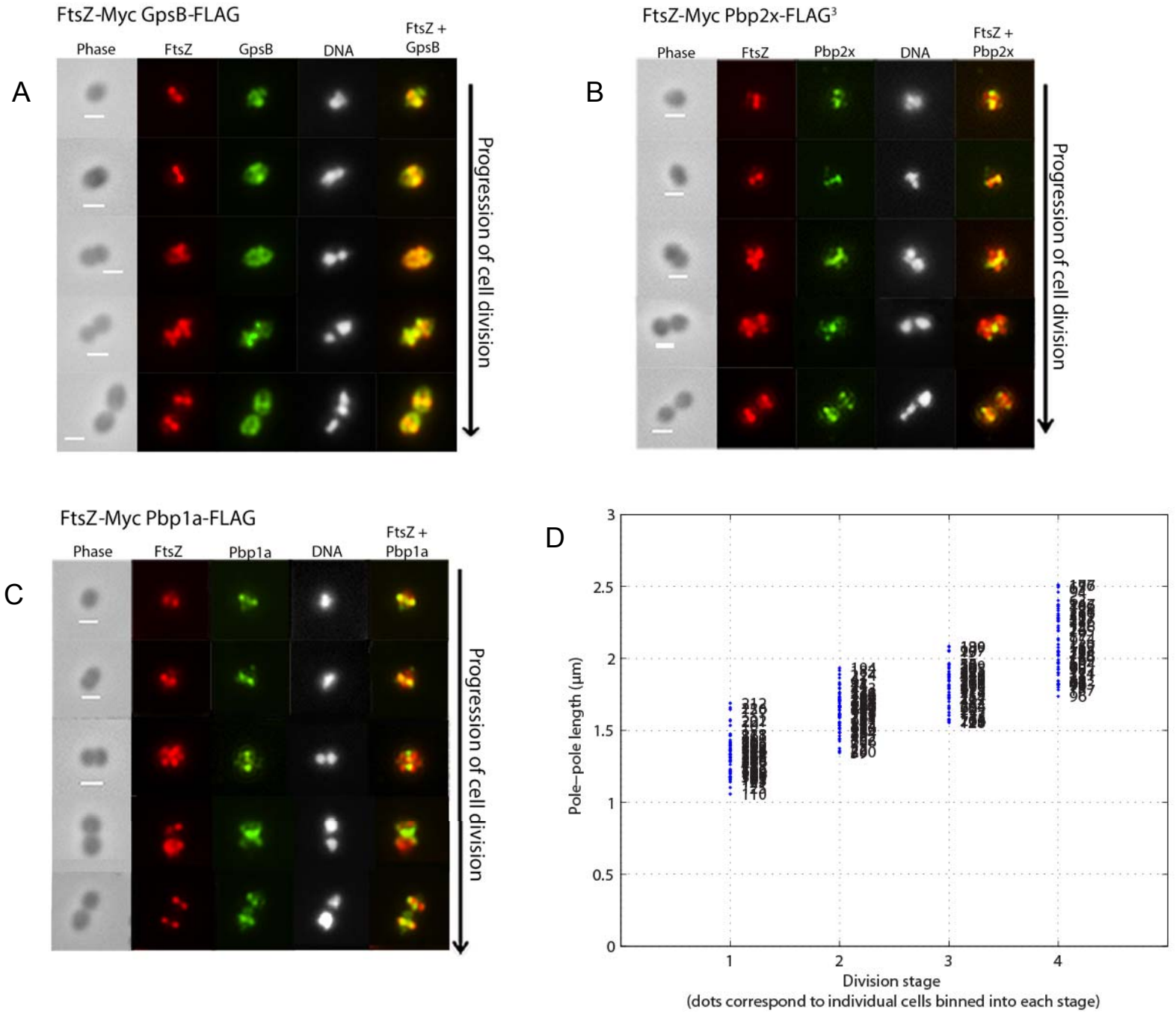
A
FtsZ-Myc GpsB-FLAG
Phase
FtsZ
GpsB
DNA
FtsZ + GpsB
Progression of cell division
B
FtsZ-Myc Pbp2x-FLAG[3]
Phase
FtsZ
Pbp2x
DNA
FtsZ + Pbp2x
Progression of cell division
C
FtsZ-Myc Pbp1a-FLAG
Phase
FtsZ
Pbp1a
DNA
FtsZ + Pbp1a
Progression of cell division
D
Pole–pole length (µm)
0
0.5
1
1.5
2
2.5
3
1
2
3
4
Division stage
(dots correspond to individual cells binned into each stage)

Fig. S7

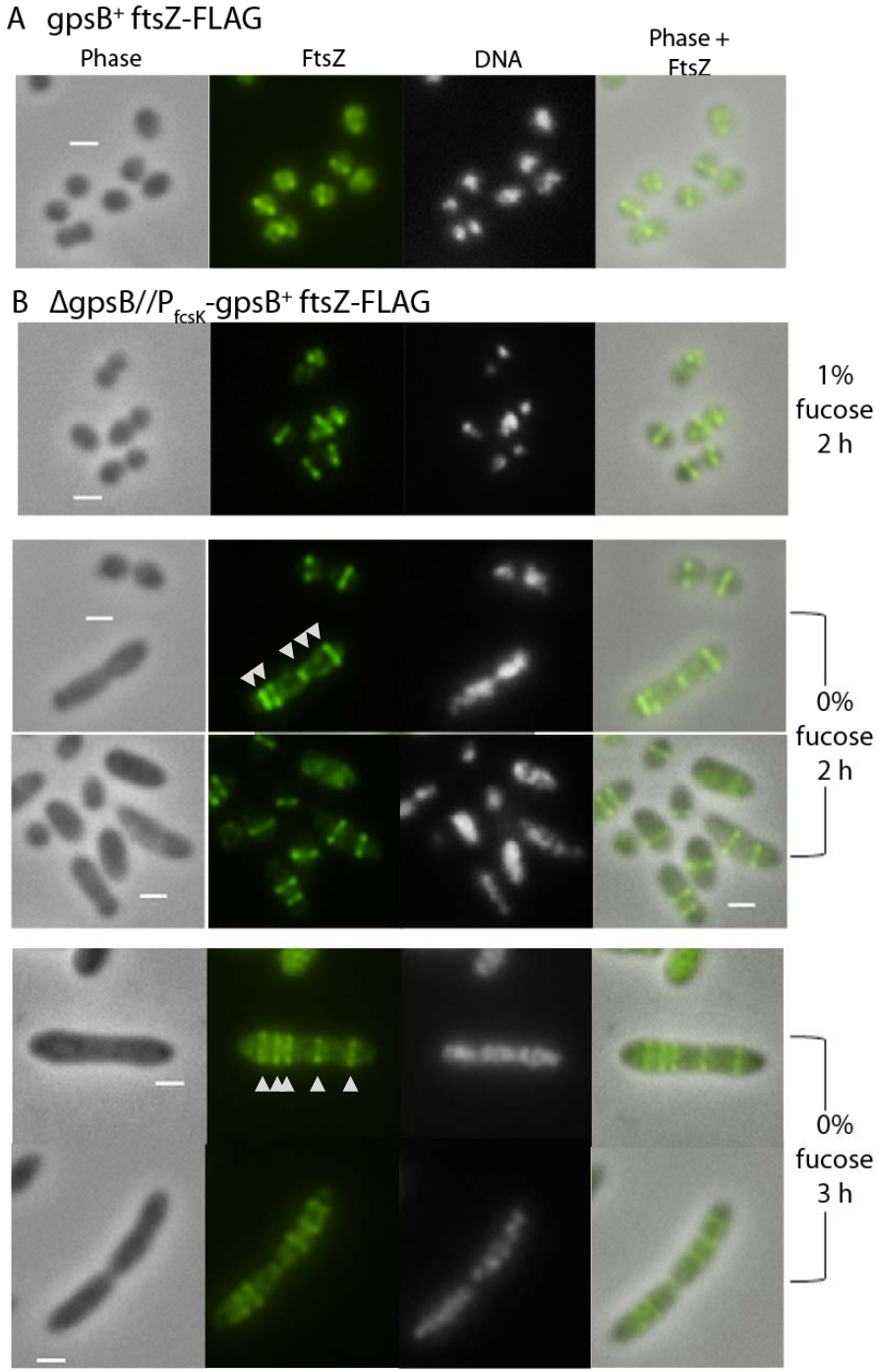
A gpsB+ ftsZ-FLAG
Phase
FtsZ
DNA
Phase + FtsZ
B ΔgpsB//PfcsK-gpsB+ ftsZ-FLAG
1% fucose 2 h
0% fucose 2 h
0% fucose 3 h

Fig. S8

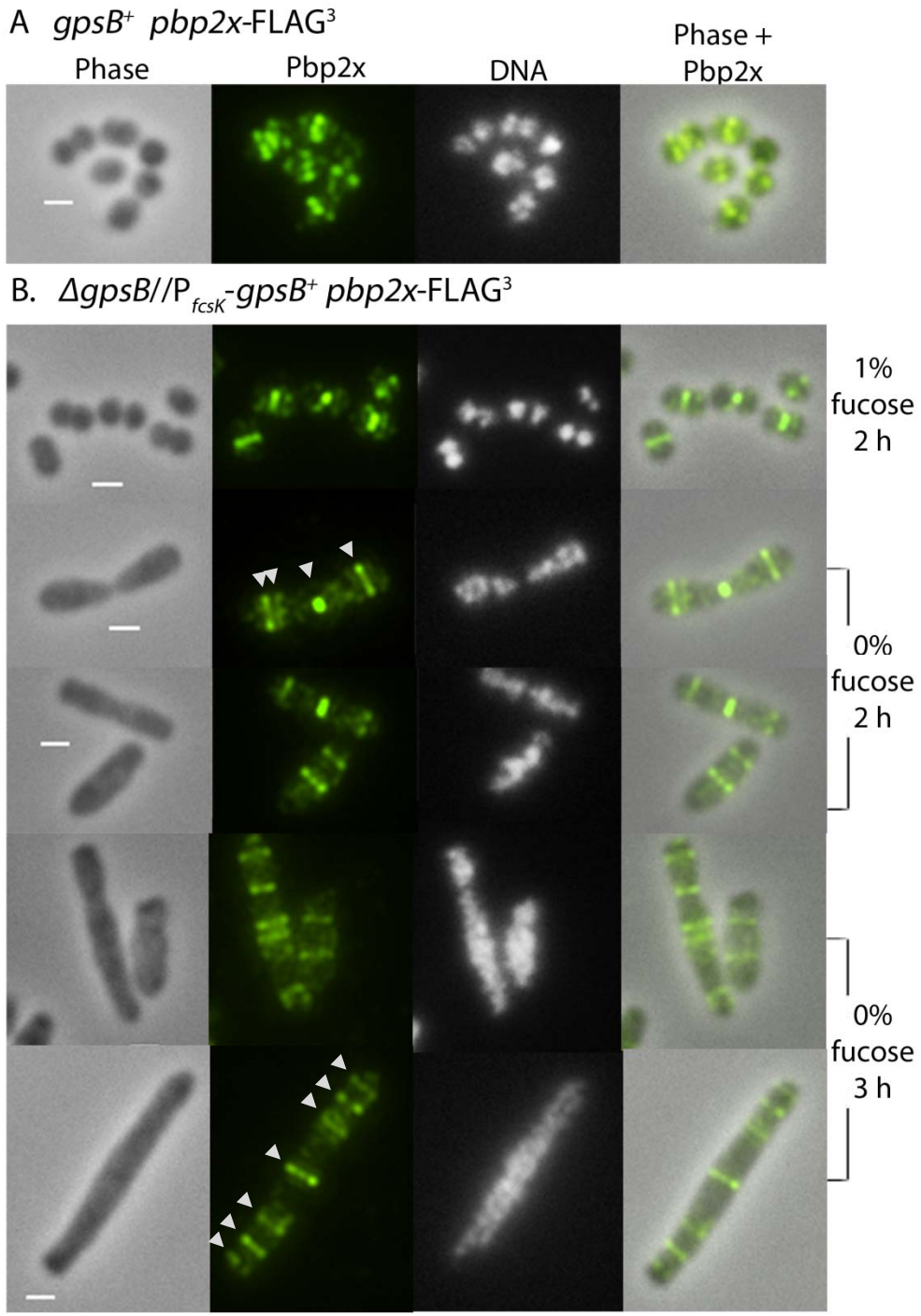
A gpsB+ pbp2x-FLAG3
Phase
Pbp2x
DNA
Phase + Pbp2x
B. ΔgpsB//P fcsK-gpsB+ pbp2x-FLAG3
1% fucose 2 h
0% fucose 2 h
0% fucose 3 h

Fig. S9

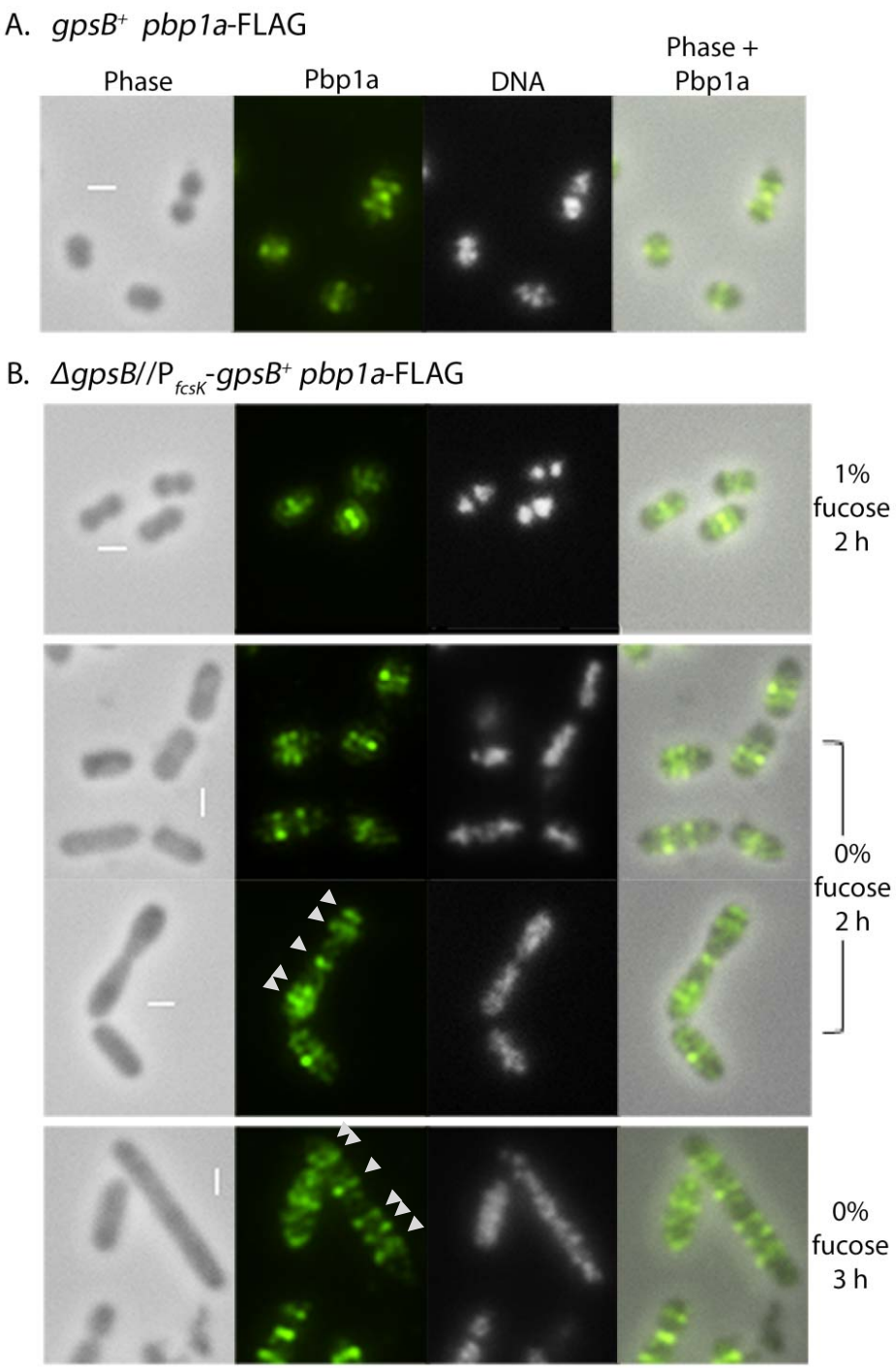
A. gpsB+ pbp1a-FLAG
Phase
Pbp1a
DNA
Phase + Pbp1a
B. ΔgpsB//PfcsK-gpsB+ pbp1a-FLAG
1% fucose 2 h
0% fucose 2 h
0% fucose 3 h

Fig. S10

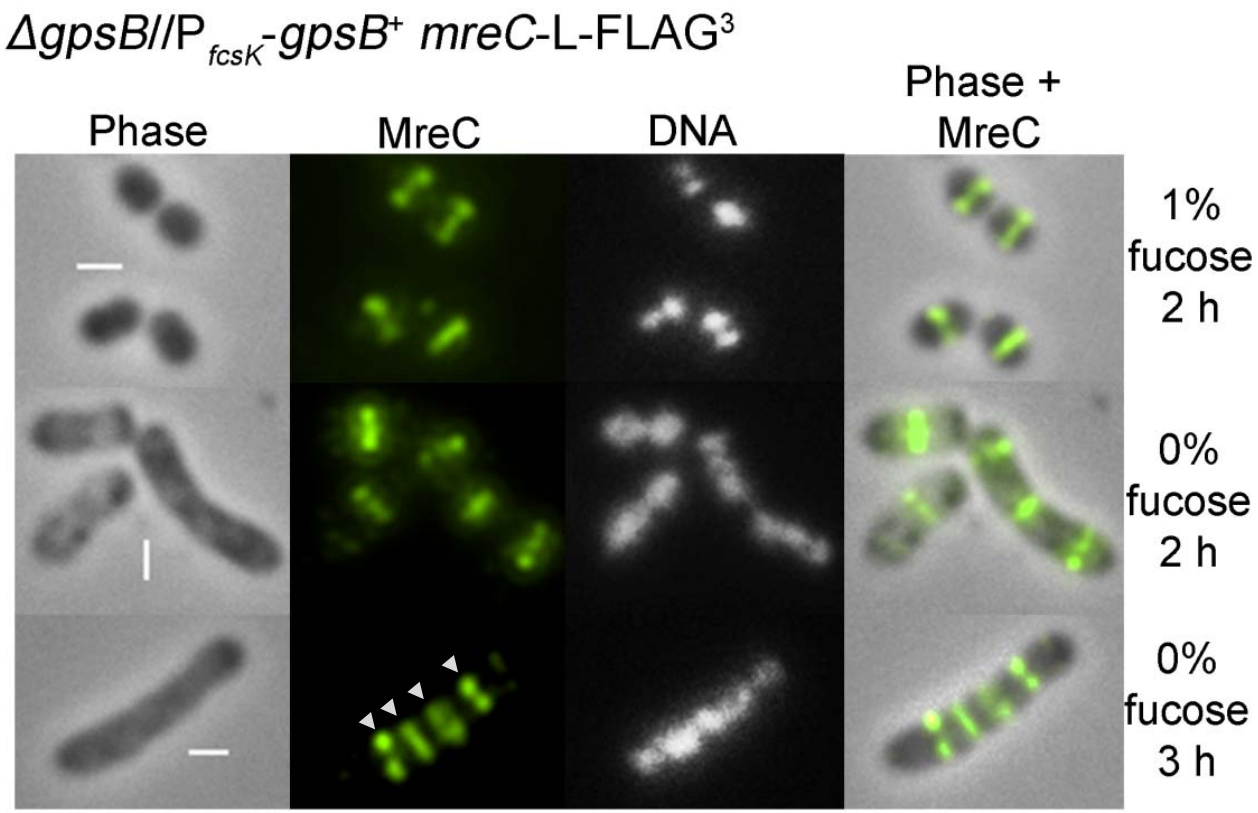
ΔgpsB//P fcsK -gpsB+ mreC-L-FLAG3
Phase
MreC
DNA
Phase + MreC
1% fucose 2 h
0% fucose 2 h
0% fucose 3 h

Fig. S11